Three Response Optimization of Spot-Welded Joint Using Taguchi Design and Response Surface Methodology Techniques

F. A. Ghazali, Z. Salleh, Yupiter H. P. Manurung, Y. M. Taib, Koay Mei Hyie, M. A. Ahamat and S. H. Ahmad Hamidi

Abstract One of the main challenges in correlating welding parameters and weld quality is its complexity to include as many as possible factors. In this research, the effects of spot welding parameters on weld quality were investigated. The effects of weld time, weld current, and electrode force on the sizes of fusion zone and heat affected zone, and tensile-shear load were studied. These welding parameters and weld quality were analysed using the three response Taguchi L_9 orthogonal array method in Minitab 17. Second-order regression models of fusion zone size, heat affected zone size and tensile-shear load were constructed by adapting Response Surface Method. The optimum weld time was 0.2 s, weld current of 10 kA and the required electrode force was 2.3 kN. These parameters were within 5% discrepancies with the experiment results. Weld current was the most important welding parameter that determines the weld quality, with the contribution of 69%. From our observation, the failure mode was the pullout type, a generally accepted failure for welded joint. The outcomes of this research contributed to the advancement in optimization technique for RSW joint, by increased the number of weld quality from two to three response.

Keywords Three response optimization · Taguchi method · Response surface methodology · Spot weld

F. A. Ghazali (✉) · M. A. Ahamat · S. H. Ahmad Hamidi
Universiti Kuala Lumpur, 1016, Jalan Sultan Ismail, 50250 Kuala Lumpur, Malaysia
e-mail: farizahadliza@unikl.edu.my

Z. Salleh · Y. H. P. Manurung · Y. M. Taib
Faculty of Mechanical Engineering, Universiti Teknologi MARA (UiTM), 40000 Shah Alam, Selangor, Malaysia

K. M. Hyie
Faculty of Mechanical Engineering, Universiti Teknologi MARA (Pulau Pinang), 13500 Permatang Pauh, Pulau Pinang, Malaysia

1 Introduction

Resistance spot welding (RSW) is a rapid joining technique to join thin shell assemblies, such as components in automotive industry. One single typical car body consists about three hundred sheet metal parts, joined by thousands of spot-weld. The strength of these joints solely relies on the quality of its weld. Therefore, it is important to use appropriate setting of parameters in RSW. Those parameters are weld current, weld time, electrode force and holding time [1]. Use of correct values for these parameters is critical to obtain the optimal quality of weld joint. In brief, these parameters will affect the sizes of fusion zone (FZ) and heat affected zone (HAZ), mechanical properties and fatigue life of a welded joint. However, the correlations between the RSW parameters and weld quality are very scarce.

Low-carbon steel is one of the commonly used materials in various industries. Thus, it is essential to understand the behaviour of low-carbon steel that undergoes RSW joining technique. Numerous researches have been conducted on the RSW of low-carbon steel; but no attempt had been made to correlate the effect of RSW parameters to three welded joint quality. Earlier researches only studied the effect of one parameter (e.g. weld current) on the specific joint quality (e.g. size of fusion zone). By neglecting other RSW joint quality, the integrity of the welded joint is debateable. Since most of industrial applications involving RSW low-carbon steel requires a good quality welded joint, a study on three-response optimization become a necessity.

The effect of four RSW parameters, namely weld current, weld time, electrode force, and holding time on tensile-shear strength of welded joint was investigated [2]. Artificial neural network was adapted to investigate the correlation between these parameters and the tensile shear strength of the joint. The sizes of fusion zone and heat affected zone were not investigated. The effect of welding parameters on the tensile shear strength for the spot-weld joint of galvanized steel sheets was reported by Thakur et al. [3]. In their work, they used Analysis of Variance (ANOVA) to evaluate the level of importance for each welding parameters. Again, only one welded joint quality was considered in [3].

An improvement on the number of welded joint quality based on fusion Zone and heat affected zone was recently published [4]. The RSW parameters were optimised using the multiple-objective quality method. Another study reported the correlation between weld current, weld time and electrode force on tensile shear strength and fusion zone using Taguchi method to determine the optimum RSW parameters [5].

An optimal resistance spot welding parameters for a 1.0 mm thickness low carbon steel by considering multi-welded joint quality was reported in [6]. The setting of welding parameters was determined using L_9 Taguchi orthogonal array experimental design method, yielded the optimal processing conditions for spot welded of low carbon steel. The optimum welding parameter for two responses was obtained using multi-signal to noise ratio (MSNR) and the significant level of the welding parameters was further analysed using analysis of variance technique.

In this paper, the welding parameters were optimized based on three-response of welded joint (fusion zone, heat affected zone and tensile-shear load) by adapting Taguchi L_9 orthogonal array and central composite design method. RSW samples were prepared based on 29 parameters combinations. The response surface methodology was used to construct the second-order correlations between fusion zone, heat affected zone and tensile-shear load and welding parameters which were validated by comparison of predicted and experiment results. The mode of failure was evaluated to determine the integrity of these welded joints.

2 Methodology

This section presents the method on preparation of low-carbon steel RSW samples, measurement methods of the sizes of fusion and heat affected zones and the tensile-shear load test procedure. The Taguchi L_9 orthogonal array and Central Composite Design methods were used in the selection of values of welding parameters.

2.1 RSW Samples Preparation and Equipment

The low-carbon steel sheet with a thickness of 1.2 mm was cut into 105 mm × 45 mm piece, in accordance to the AWS 8.9 m standard. Then, two pieces of 105 mm × 45 mm × 1.2 mm sheet was welded using JPC 75 kVa spot welder machine in a single lap shear joint type, with the overlap of 35 mm. The machine was set to AC waveform, and the 5 mm diameter electrode was truncated at 30°. The chemical composition of the low-carbon steel is available in Table 1.

2.2 RSW Parameters Selection

The range of welding parameters as recommended in the manufacturer datasheet of JPC 75 kVa spot welder machine are available in Table 2. These data were used as the upper and lower limits of welding parameters.

For the Taguchi L_9 orthogonal array optimization method, the welding parameters and their factor levels are presented in Table 3. The values used for Level 2 were taken

Table 1 Chemical composition (%) of low carbon steel [7]

C	S	Mn	P	S	Fe
0.05	0.01	0.21	0.011	0.005	Bal.

Table 2 Range of welding parameters [8]

Variable	Range
Weld time (s)	0.17–0.31
Electrode force (kN)	2.0–3.4
Weld current (kA)	7.3–10.7

Table 3 Welding parameters and their factor levels for Taguchi L_9 orthogonal array

Symbol	Welding parameter	Unit	Level 1	Level 2	Level 3
WT	Weld time	s	0.2	0.24	0.28
EF	Electrode force	kN	2.3	2.7	3.1
WC	Weld current	kA	8.0	9.0	10.0

Table 4 Combinations of factor level in Taguchi L_9 orthogonal array

Experiment number	Factor level		
	WT	EF	WC
1	1	1	1
2	2	1	2
3	3	1	3
4	1	2	2
5	2	2	3
6	3	2	1
7	1	3	3
8	2	3	1
9	3	3	2

Table 5 Parameters and levels applied in CCD for spot weld of low carbon steel

Symbol	Parameter	Unit	Level				
			$-\alpha$	-1	0	$+1$	$+\alpha$
WT	Weld time	s	0.17	0.20	0.24	0.28	0.31
EF	Electrode force	kN	2.0	2.3	2.7	3.1	3.4
WC	Weld current	kA	7.3	8	9	10	10.7

from the average of maximum and minimum values for each variables in Table 2. In Table 4, nine combinations of factor level for welding parameters are specified.

The Central Composite Design (CCD) method was adapted to construct the second-order model to correlate welding parameters and welded joint quality. Five levels were used in CCD, and the values of parameters were tabulated in Table 5. A total of 20 parameters combinations were tested through experiments (Table 8).
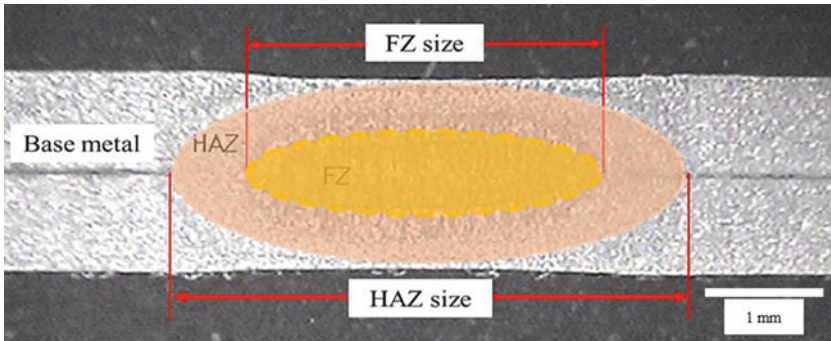
Fig. 1 Typical macrograph of weld zones

2.3 Measurement of FZ and HAZ Sizes

The welded sample was cut transversely at its center line using a cutter blade to expose its fusion zone and heat affected zone. Then, the surface was etched using 2% Nital solution for 5 s at room temperature. The macrograph of weld zone was captured using a zoom stereo microscope (Olympus BX 41 M Microscope) equipped with an image analysis system (IMAPS Version 4.0 Professional Edition Software). The typical shape of macrograph of weld zone, fusion zone, and heat affected zone is shown in Fig. 1.

2.4 Evaluation of Tensile-Shear Load

For tensile-shear load test, the tests were conducted according to the ISO 14323 standard. An Instron 200 kN universal testing machine was used to execute the tensile-shear load test. The crosshead rate was set at 2 mm/min. Three samples were prepared for each combination of RSW parameters, and the average tensile-shear load was taken for comparison with the calculated value from the second-order model that was constructed from CCD experiments results. After the samples failed, its failure modes were classified into interfacial and nugget pullout by visual inspection.

3 Results and Discussion

In this section, the findings on Taguchi L_9 OA and CCD optimization methods, and the failure mode of RSW sample are presented.

3.1 Three-Response Taguchi

The results of the experiments using Taguchi L_9 orthogonal array for FZ size, HAZ size and tensile-shear load is depicted in Table 6. The size of FZ was between 3.05 and 3.50 mm while the HAZ size was between 4.09 and 4.34 mm. For the tensile-shear load, the highest was 8.82 kN.

The results of analysis of variance (ANOVA) for the welding responses in Table 6 are presented in Table 7. ANOVA technique enables the evaluation of significant factors in three-response optimization for FZ size, HAZ size, and tensile-shear load. The value of F ranks the magnitude of influence of welding parameters on the weld-joint quality. A parameter with a higher value of F has more influence on the welded joint quality [9]. In our work, weld current is the most significant welding parameters affecting the welded joint quality whereas weld time has the lowest significance.

A further analysis confirmed that the most important factor is the weld current with 68.68%, a 44% more than the electrode force. The weld time has the lowest contribution of 6.43%. In short, a higher percentage of contribution means the parameter has more influence on the welded joint quality. Our results agreed with [6, 10], where weld current is the most important parameter in RSW. It was estimated that the

Table 6 Weld quality for Taguchi L_9 orthogonal array

Experiment number	FZ size (mm)	HAZ size (mm)	Tensile-shear load (kN)
1	3.05	4.14	7.89
2	3.06	4.41	7.84
3	3.06	4.19	8.50
4	3.32	4.28	8.43
5	3.34	4.34	8.55
6	3.36	4.32	8.53
7	3.36	4.26	8.48
8	3.41	4.19	8.48
9	3.50	4.09	8.82

Table 7 Results of ANOVA for the significance of welding parameters

Welding parameter	DF	Sum of squares	Mean of squares	F	P	Contribution
Weld time	2	4.851	2.4255	12.59	0.006	6.43
Weld current	2	51.811	25.9055	134.45	0.042	68.68
Electrode force	2	18.876	9.388	48.72	0.011	24.89
Error	2	0.146	0.073			
Total	8	75.854				100

variance for these experiments was 0.146, an indicator of an acceptable experiment design.

From the statistical point of view, the variables that have p-value that is less than 0.05 is considered statistically significant to the welded joint quality. The analysis showed that weld time, weld current and electrode force were all significant in determining the welded joint quality. All of these weld parameters were considered in the developed response surface model reported in Sect. 3.2.

3.2 Response Surface Methodology

The second order response surface model for the significant parameters affecting the FZ size, HAZ size and tensile-shear load was constructed using the three responses Taguchi L_9 orthogonal array method. The CCD (Central Composite design) technique was used to generate 20 combinations of welding parameters (Table 8). The combinations were based on 8 factorial points (standard order 1–8), six star points (standard order 9–14) and six replicates of the center point (standard order 15–20).

The design was expanded to evaluate several points which increased the chance in detecting the response at which the optimum parameters combinations occurred. The center point represented a set of experiment conditions at which six independent replicates were run. The variation between those conditions reflected the variability of all designs. It was used to estimate the standard deviation. All optimization experiments were conducted randomly in one block of measurement.

A second-order model for FZ, HAZ and tensile shear load was constructed to describe the behavior of each response. The second-order models for the FZ size, HAZ size and tensile-shear load in terms of un-coded variables with all significant terms are given in Eqs. (1)–(3), respectively:

$$
\begin{aligned}
FZ = {}&3.61 + 0.15WT + 0.08EF + 0.15WC - 0.13WT^2 \\
&+ 0.03EF^2 - 0.04WT * EF - 0.07WT * WC + 0.02EF * WC
\end{aligned} \tag{1}
$$

$$
\begin{aligned}
HAZ = {}&4.68 + 0.12WT + 0.07EF + 0.05WC - 0.06WT^2 + 0.03EF^2 \\
&- 0.02WC^2 - 0.06WT * EF - 0.04WT * WC + 0.07EF * WC
\end{aligned} \tag{2}
$$

$$
\begin{aligned}
\text{Tensile-shear load} = {}&8.62 + 0.45WT + 0.28EF \\
&+ 0.23WC - 0.22WT^2 - 0.03EF^2 - 0.03WC^2 \\
&- 0.20WT * EF - 0.27WT * WC + 0.11EF * WC
\end{aligned} \tag{3}
$$

The analysis showed that the regression model and each variable term (linear, square and interaction) in the model had a p-value that was less than 0.05. To test the global fit of the model, the coefficient of determination (R^2) was evaluated. The R^2 for tensile-shear load was 0.997, denoting that the sample variation of 99.7% is attributed to the regressors in the model and only 0.3% of the total variability is

Table 8 Design matrix of CCD and experimental design

Run order	Parameter			Response		
	Weld time (s)	Weld current (kA)	Electrode force (kN)	FZ size (mm)	HAZ size (mm)	Tensile-shear load (kN)
1	0.24	9	2.7	3.61	4.68	8.63
2	0.24	9	2.7	3.60	4.69	8.67
3	0.20	8	2.3	3.02	4.32	7.01
4	0.28	10	2.3	3.74	4.65	8.50
5	0.24	10.7	2.7	3.81	4.70	8.96
6	0.20	10	3.1	3.79	4.80	8.96
7	0.28	8	2.3	3.40	4.77	8.88
8	0.24	9	2.0	3.58	4.68	8.13
9	0.24	9	2.7	3.62	4.66	8.59
10	0.20	8	3.1	3.11	4.50	7.80
11	0.24	7.3	2.7	3.48	4.56	8.15
12	0.24	9	2.7	3.62	4.66	8.58
13	0.17	9	2.7	3.05	4.34	7.24
14	0.20	10	2.3	3.29	4.40	7.80
15	0.24	9	3.4	3.74	4.84	8.98
16	0.31	9	2.7	3.50	4.71	8.78
17	0.28	8	3.1	3.66	4.68	8.80
18	0.24	9	2.7	3.61	4.69	8.60
19	0.24	9	2.7	3.60	4.68	8.65
20	0.28	10	3.1	3.72	4.88	8.96

not explained by the model. The R^2 for the FZ size and HAZ size were 90.71 and 97.78%, respectively.

3.3 Confirmation Tests

The results obtained from Eqs. (1) to (3) were compared with the experiments (Table 9). The percentage of discrepancies between confirmation experiments and prediction (Eqs. 1–3) were less than 3.7%. From the ANOVA analysis, the optimum welding parameters are as follow: weld time of 0.2 s, electrode force at 2.3 kN and a weld current of 10 kA.

The investigation on failure mode was carried out using tensile-shear test until the welded joint was failed. The failure was classified either as the well button pullout or interfacial fracture. For the RSW joint of the samples, it was observed that the failure mode was a pullout failure as in Fig. 2. This type of failure is generally the preferred

Table 9 Results of the confirmation tests for FZ size, HAZ size and tensile-shear load

Parameter	Value from Eqs. (1) to (3)	Experiment				Discrepancy (%)
		1	2	3	Average	
FZ size (mm)	3.50	3.49	3.41	3.43	3.44	1.71
HAZ size (mm)	4.54	4.63	4.55	4.58	4.59	1.09
Tensile-shear load (kN)	8.52	8.02	8.13	8.47	8.21	3.64

failure mode in resistance spot welding, due to its higher plastic deformation and energy absorption characteristics [11–13].

For a welded joint, the failure usually occurs at the softer base metal. The samples tested in this work produced the complete button pullout. In the pullout mode, failure commonly occurs via withdrawal of fusion zone (Fig. 2a) from one of the sheets [14, 15]. One of the signs of insufficient mechanical strength in RSW joint is if the failure occurs in the mode of interfacial failure or through the fusion zone failure [16].

In Fig. 2b, the failure of the spot weld appears to be initiated approximately at the middle of the fusion zone circumference before it was propagated through necking/shear along the fusion zone circumference. Once the welded joint lost its strength, the upper sheet was torn off. This observed failure mechanism is in agreement with other literatures [15, 17]. It can be concluded that the strength of weld joint produced by the combination of optimized parameters were able to create a joint with an acceptable failure mode.

4 Conclusions

An experimental design using a three-response optimization using the Taguchi L_9 orthogonal array method was used to determine the effects of welding parameters (weld time, weld current and electrode force) on the fusion zone size, heat affected zone size and tensile-shear load, simultaneously. Three second-order models for fusion zone size, heat affected zone size and tensile-shear load were constructed and validated by comparing the predicted values and experiment results. These second-order models were satisfactory since the values of R^2 for the global fitting of fusion zone size, heat affected zone size, and tensile-shear load were 0.907, 0.9778 and 0.994, respectively. It was found that the weld time of 0.2 s, electrode force at 2.3 kN and a weld current of 10 kA produced the desired welded joint quality. The experimental results obtained using these optimum welding parameters and the prediction based on the second-order models were within 3.7% discrepancies.

Fig. 2 Failure mode of
tensile-shear test **a** pullout
and **b** tearing

(a)

(b)
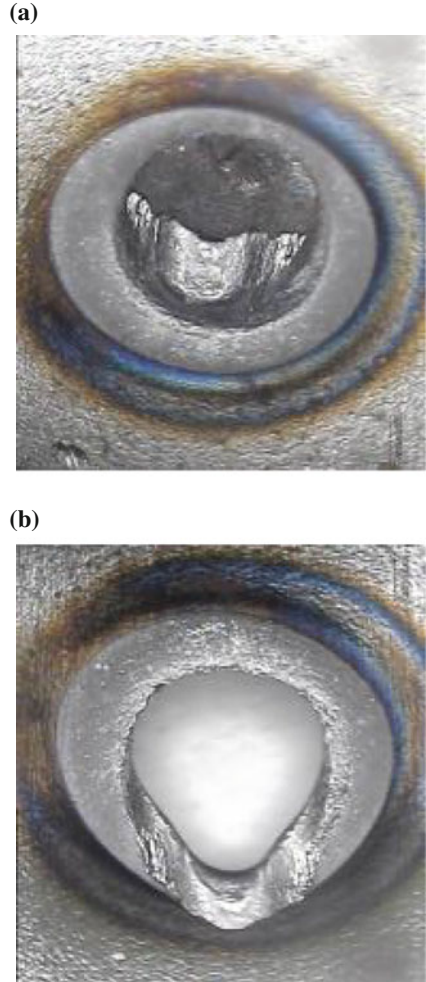
References

1. Muhammad N, Manurung YHP (2012) Design parameter selection and optimization of weld zone development in resistance spot welding. World Acad Sci Eng Technol 71
2. Hamidinejad SM, Kolahan AF, Kokabi AH (2012) The modeling and process analysis of resistance spot welding on galvanized steel sheets used in car body manufacturing. Mater Des 34:9
3. Thakur AG, Rao T, Mukhedkar MS, Nandedkar VM (2010) Application of Taguchi method for resistance spot welding of galvanized steel. ARPN J Eng Appl Sci 5(11):5
4. Muhammad N, Manurung YHP, Jaafar R, Abas SK, Tham G, Haruman E (2013) Model development for quality features of resistance spot welding using multi-objective Taguchi method and response surface methodology. J Intell Manuf 24:1175–1183

5. Pandey AK, Moeed KM, Khan MI (2013) Investigation of the effect of current on tensile strength and nugget diameter of spot welds made on AISI-1008 steel sheets. Int J Tech Res Appl 1:8

6. Muhammad N, Manurung YHP, Hafidzi M, Abas SK, Tham G, Rahim MRA (2012) A quality improvement approach for resistance spot welding using multi-objective Taguchi Method and response surface methodology. Int J Adv Sci Eng Inf Technol 2:6

7. Ghazali FA, Manurung YHP, Mohamed MA (2014) Multi-response optimization using Taguchi method of resistance spot welding parameters, Appl Mech Mater 660

8. Ghazali FA, Berhan MN, Manurung YHP, Salleh Z, Abdullah S (2015) Tri-objective optimization of carbon steel spot-welded joints. J Teknol 76(11)

9. Ahmadi H, Arab NBM, Ghasemi FA (2014) Optimization of process parameters for friction stir lap welding of carbon fibre reinforced thermoplastic composites by Taguchi method. J Mech Sci Technol 28(1):279–284

10. Esme U (2009) Application of Taguchi method for the optimization of resistance spot welding process. Arab J Sci Eng 34

11. Pouranvari M, Marashi SPH (2010) On the failure of low carbon steel resistance spot welds in quasi-static tensile–shear loading. Mater Des 31(8):3647–3652

12. Abadi MMH, Pouranvari M (2010) Correlation between macro/micro structure and mechanical properties of dissimilar resistance spot weld of AISI 304 Austenitic stainless steel and AISI 1008 low carbon steel. Assoc Metall Eng Serbia AMES 16(2):14

13. Pouranvari M, Ranjbarnoodeh E (2011) Resistance spot welding characteristic of ferrite-martensite DP600 dual phase advanced high strength steel-part II: failure mode. World Appl Sci J 15(11):1527–1531

14. Pouranvari M (2011) Effect of welding parameters on the peak load and energy absorption of low-carbon steel resistance spot welds. Int Sch. Res Netw ISRN Mech Eng 2011:1–7

15. Marashi P, Pouranvari M, Amirabdollahian S, Abedi A, Goodarzi M (2008) Microstructure and failure behavior of dissimilar resistance spot welds between low carbon galvanized and austenitic stainless steels. Mater Sci Eng, A 480:5

16. Jahandideh A, Hamedi M, Mansourzadeh S, Rahi A (2011) An experimental study on effects of post-heating parameters on resistance spot welding of SAPH440 steel. Sci Technol Weld Join 16(8):669–675

17. Pouranvari M, Marashi P (2009) Failure behaviour of resistance spot welded low. Assoc Metall Eng Serbia AMES 15(3):8